Use of chloroethylene carbonate as an electrolyte solvent for a graphite anode in a lithium-ion battery

Shu, Z. X.; McMillan, Roderick; Murray, J. J.; Davidson, Isobel

Publisher's version / Version de l'éditeur:
https://doi.org/10.1149/1.1836985
Journal of the Electrochemical Society, 143, July 7, pp. 2230-2235, 1996

16. I. Saeki, H. Konno, and R. Furuichi, *Corros. Sci.*, **38**, 19 (1996).
17. G. Hodes, D. Cahen, and J. Manassen, *Nature*, **260**, 312 (1976).
18. F. Di Quarto, A. Di Paola, and C. Sunseri, *Electrochim. Acta*, **26**, 1177 (1981).
19. *Semiconductor Electrodes*, Harry O. Finklea, Editor, p. 71, Elsevier, Amsterdam (1988).
20. *Atlas d'Equilibres Electrochimiques*, M. Pourbaix, Editor, p. 280, Gauthier-Villars, Paris (1963).
21. *High Temperature Oxidation of Metals*, P. Kofstad, Editor, p. 251, John Wiley & Sons, New York (1966).

Use of Chloroethylene Carbonate as an Electrolyte Solvent for a Graphite Anode in a Lithium-Ion Battery

Z. X. Shu,* R. S. McMillan,* J. J. Murray, and I. J. Davidson

Institute for Environmental Research and Technology, National Research Council Canada, Ottawa, Ontario, Canada K1A OR6

ABSTRACT

The electrolyte decomposition during the first lithiation of graphite is reduced to 90 mAh/g in an electrolyte containing equal volumes of chloroethylene carbonate and a cosolvent of propylene carbonate, dimethyl carbonate, or diethyl carbonate. The volume fraction of chloroethylene carbonate can be further reduced to 0.05 in a trisolvent system with a cosolvent containing equal volumes of ethylene carbonate and propylene carbonate. A lithium-ion cell containing chloroethylene carbonate and propylene carbonate shows a long cycle life. The capacity decreases by 20% from the initial value in over 800 cycles. The charging efficiency is 80 to 90%, is rate dependent, and is accompanied by a self-discharge mechanism. A hypothesis of a chemical shuttle is suggested to explain the low charge efficiency and self-discharge.

Introduction

In the past decade, there has been a growing interest in the search for suitable carbon materials as an intercalation host (anode) for lithium-ion rechargeable batteries. Graphite has been considered as a favorable candidate because of its high capacity and low and flat potential curve with respect to lithium metal. A major problem in using graphite as the anode is the massive electrolyte decomposition during the first lithiation process, at least in a propylene carbonate (PC) based electrolyte.[1-3] This necessitates the presence of both excess lithium and electrolyte sources in the cell and reduces the apparent cell capacity.

Several approaches[4-7] have been explored in the past to reduce the extent of electrolyte decomposition at the graphite electrode. Two of the promising electrolytes among these are $LiPF_6$ in ethylene carbonate/dimethyl carbonate (EC/DMC) or in ethylene carbonate/diethyl carbonate (EC/DEC). However, $LiPF_6$ is relatively expensive and unstable in the solid form under moderate heat and moisture levels.

Recently, we reported preliminary results using chloroethylene carbonate as an electrolyte solvent.[8,9] This electrolyte may also contain propylene carbonate as a cosolvent. Our results showed that this PC-based electrolyte could be used with a highly graphitic electrode and did not incur an excessive amount of electrolyte decomposition. This paper presents additional results for this electrolyte system and preliminary results obtained from a trisolvent system.

Experimental

For a bisolvent system, the electrolyte was 1 *M* $LiClO_4$ (Baker) or 1 *M* $LiPF_6$ (Hashimoto) dissolved in a mixture of chloroethylene carbonate (Chloro-EC) and a cosolvent of propylene carbonate (PC), diethyl carbonate (DEC), dimethyl carbonate (DMC), 2-methyl tetrahydrofuran (2Me-THF), tetrahydrofuran (THF), or tetrahydropyran (THP). For a trisolvent system, the electrolyte was 1 *M* $LiClO_4$ dissolved in Chloro-EC, ethylene carbonate (EC), and PC where EC and PC were kept at an equal volume ratio. $LiClO_4$ was dried under vacuum at 120°C overnight. $LiPF_6$ was used as received without further purification. All electrolyte solvents were dried over activated molecular sieves followed by distillation. In the case of Chloro-EC, EC, and PC, distillation was carried out under vacuum. The water content of the electrolyte was measured using Karl-Fisher titration and was less than 50 ppm.

The carbon electrode was made of KS series Lonza artificial graphite. KS15 [14 m^2/g by Brunauer, Emmett, and Teller method (BET)], was used predominantly. The electrode contained 3 to 5% vinylidene fluoride resin (Elf Atochem). It was prepared using the method described previously.[3,8] Typically, the electrode density was 0.6 g/cm^3.

Experiments were carried out using a two-electrode cell. The cell capacity was limited by that of the graphite electrode in both Li/graphite and graphite/$LiCoO_2$ cell configurations. The theoretical cell capacity was calculated assuming 1 mole of lithium intercalated per 6 moles of graphite (*i.e.*, LiC_6).

In a lithium/graphite cell, the anode was lithium metal (Foote), and the cathode was graphite. In a lithium-ion cell, the anode was graphite, and the cathode was $LiCoO_2$ (Johnson-Matthey). The cathode also contained 10% carbon black (Super S, S. Ensagri-Willebroek N. V.) and 5% vinylidene fluoride resin (Elf Atochem). A few experiments were conducted where lithium metal was the anode and $LiCoO_2$ the cathode and the cathode was prepared as indicated above. In all cases, a polypropylene microporous membrane (Celgard 3501) was used as the separator. NRC designed and fabricated 2325 coin cells were used as a cell testing vehicle.

The cycling equipment was as described in Ref. 3. Unless otherwise stated, the electrochemical cells were cycled galvanostatically between potential limits of 10 mV and 2.0 V for lithium/graphite cells, 3.0 and 4.2 V for lithium/$LiCoO_2$ cells, and between 2.5 and 3.9 V for lithium-ion cells.

The experimental conditions were not optimized for maximum capacity and cycle life.

Reported cell data represent multiple experiments yielding reproducible results. Values for reversible and irreversible capacities were reproducible to ±3 and 5%, respectively.

Cyclovoltammetric experiments were performed using an EG&G Princeton Applied Research 273 potentiostat and a three-electrode cell. The working electrode was Shomac 30-2 (Showa Denko America Inc.) stainless steel or Super S carbon black (40 m^2/g by BET). The carbon black was held between two porous Shomac steel plates. A

* Electrochemical Society Active Member.

stainless steel gauze was used as the counterelectrode, and lithium metal as the reference electrode. The cell was purged with Ar at room temperature. Sweep rates between 1 and 10 mV/s were employed. Current densities are reported for 5 mV/s per geometric area.

Results and Discussions

Li/graphite cells bisolvent systems.—PC as a cosolvent.—In our previous publications,[8,9] the electrochemical behavior of the first cycle of a Li/KS15 graphite cell with 1 *M* $LiClO_4$ Chloro-EC/PC (1/1) was reported. At a 20 h rate, it was found that the capacity loss during the first cycle was 108 mAh/g, and a reversible capacity of 359 mAh/g was obtained. We attributed the capacity loss to the formation of a solid-electrolyte-interface (SEI) film[10] on the surface of graphite. Figure 1 shows comparable data for recent work. The reversible capacity is similar, but the capacity loss has been reduced to 88 mAh/g. This improvement is explained later. The potential curves shown in Fig. 1 show the vast increase in capacity loss when Chloro-EC is not present in the electrolyte.

In the present work, the electrolyte decomposition was further investigated using a series of artificial graphites with different surface areas. The experiments were carried out with 1 *M* $LiClO_4$ Chloro-EC/PC (1/1) electrolyte using Li/graphite cells. Figure 2 shows results of the first cycle for two types, (KS4 and 25), of Lonza KS series artificial graphite cells cycled at a 20 h rate. The potential curves follow a similar trend to that observed in Fig. 1. However, the extent of the electrolyte decomposition at the potential plateau of 1.2 V depends very much on the surface area of the graphite used. Comparison of the data of Fig. 1 and 2 shows that the electrolyte decomposition increases with the surface area but in a nonlinear fashion.

Fong *et al.*[11] suggested that, with a Li/graphite cell in an EC/PC (1/1) electrolyte, two electrolyte decomposition processes, one at 1.2 V and the other at 0.8 V, occurred during the first lithiation of graphite. They attributed the former to the formation of an SEI film at the graphite surface and the latter to the exfoliation of graphite. In addition, the former showed a linear relationship with the surface area whereas the latter was independent of the surface area.

In our work, EC was replaced by Chloro-EC. The potential plateau at 0.8 V, where the exfoliation of graphite was suggested to occur with an EC/PC-based electrolyte, was completely absent. The plateau at about 1.2 V remained. We attribute this plateau to the formation of an SEI film as suggested by Fong *et al.*[11] We do not fully understand the nature of the film at the present time (see below for further discussion). Nevertheless, the film formed from the decomposition of Chloro-EC is sufficiently stable to protect the graphite from exfoliation in the presence of PC. This is evidenced by the fact that the plateau at 0.8 V with

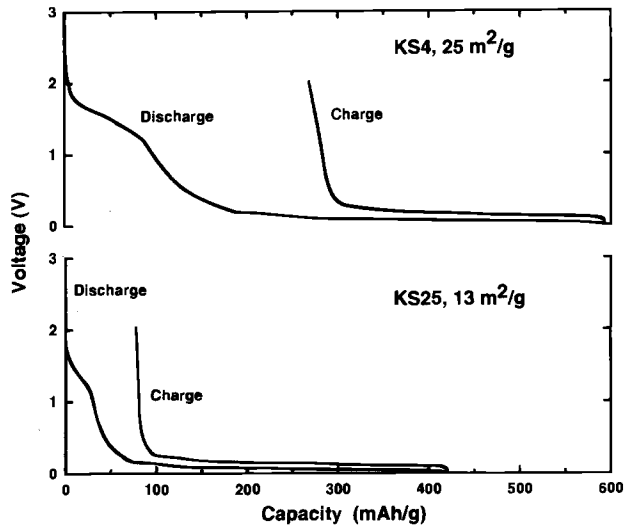

Fig. 2. Potential profiles of the first cycle of Li/graphite cells employing 1 *M* $LiClO_4$ Chloro-EC/PC (1/1) electrolyte and cycled at a 20 h rate. The type and BET surface area of the graphite are as shown.

our electrolyte is completely absent. It should be noted, however, that if the volume fraction of Chloro-EC is decreased to below the optimum value, about 0.3,[9] then the plateau at 0.8 V appears. The SEI film is formed predominantly on the first cycle of the cell. Discharge curves subsequent to the first mirror the first charge curve while charge curves mimic it. The charge efficiency, defined as the discharge capacity divided by the subsequent charge capacity multiplied by 100%, becomes greater than 98% within four cycles.

Rate capacity.—Figure 3 shows the reversible cell capacity as a function of the cycling rate with 1 *M* $LiClO_4$ Chloro-EC/PC (1/1) and KS15 graphite. The cell capacity decreases as the cycling rate increases but remains above 300 mAh/g at rates below 0.4 C. For rates greater than 0.4 C, the cell capacity decreases more rapidly, reaching 160 mAh/g at 0.8 C. Also shown in Fig. 3 are results for a cell made in a similar manner but containing 1 *M* $LiPF_6$ EC/DMC (1/2) as the electrolyte. This electrolyte has been used widely with a graphite anode in a lithium-ion cell.[12] Within the experimental error, there are no significant differences in capacity *vs.* cycling rate between the cell containing Chloro-EC/PC and that containing EC/DMC.

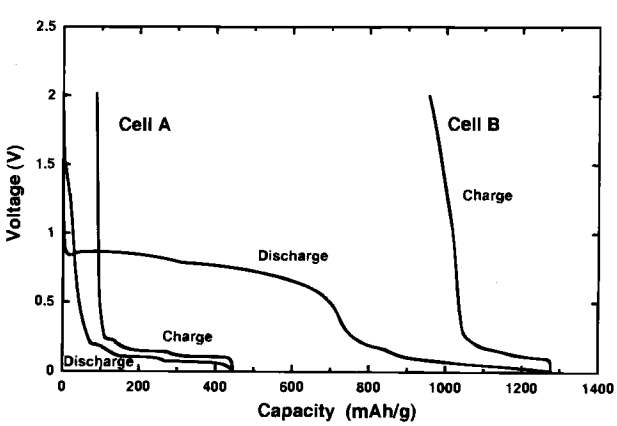

Fig. 1. Potential profiles of the first cycle of Li/KS15 graphite cells cycled at a 20 h rate. Cell A: 1 *M* $LiClO_4$ Chloro-EC/PC (1/1). Cell B: 1 *M* $LiClO_4$ EC/PC (1/1).

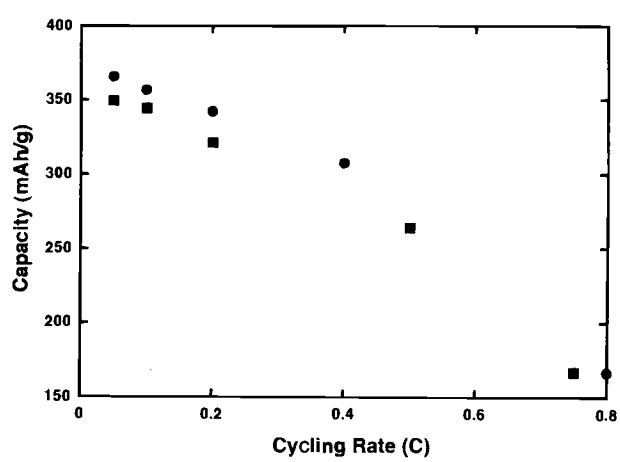

Fig. 3. Rate dependence of Li/KS15 graphite cells employing 1 *M* $LiClO_4$ Chloro-EC/PC (1/1), (●) and 1 *M* $LiPF_6$ EC/DMC (1/2), (■) electrolyte.

Electrolytes based on other solvents.—Experiments were carried out with an electrolyte 1 *M* $LiClO_4$ in Chloro-EC mixed with other conventional electrolyte solvents in a 1:1 volume ratio. Potential profiles (not shown) with these cosolvents were similar to those of Fig. 2 where PC was the cosolvent. The extent of electrolyte decomposition and reversible capacity were functions of the cosolvent. Table I lists the reversible capacity and capacity loss for the first cycle at a 20 h rate with these electrolyte systems for KS15 graphite. It is clear in terms of reversible capacity and capacity loss that DEC and DMC are comparable to PC and all three are much better than THF, THP, or 2-MeTHF. The higher irreversible capacity in ether-based electrolytes may be due to a lower stability of the SEI film in these electrolytes. When $LiClO_4$ was replaced by $LiPF_6$, similar results were obtained with PC, DEC, or DMC as a cosolvent. The capacity loss during the first cycle and reversible capacity of a cell with Chloro-EC/PC, Chloro-EC/DMC, or Chloro-EC/DEC based electrolytes are comparable to those obtained with $LiPF_6$ EC/DMC electrolyte.[8] The capacity loss for the former three are *ca.* 90 mAh/g as compared to 120 mAh/g for EC/DMC electrolyte under comparable conditions, while the reversible capacities are, respectively, *ca.* 352 and 346 mAh/g. As was indicated above, the capacity loss for PC as a cosolvent is improved from our last report.[9] This was the result of an improved control on the moisture level of various components inside the cell. Again, it is believed that the formation of a stable SEI film on the surface of graphite permits the use of PC in the electrolyte without incurring an excess amount of electrolyte decomposition.

Li/graphite cells trisolvent system.—Following the success of using PC as a cosolvent with Chloro-EC in a graphite/Li cell, the possibility of using a three-solvent system with a graphite electrode was investigated. Chloro-EC, although it has the desirable properties, is expensive. The current bisolvent system requires the volume fraction of Chloro-EC to be at least 0.3.[9] The objective here is to reduce the amount of Chloro-EC required in the system while maintaining the irreversible capacity at a level similar to those shown in Table I.

Experiments were carried out where the volume fractions of PC and EC were kept equal (*i.e.*, PC/EC volume ratio was fixed at 1:1) and the amount of Chloro-EC was varied. The potential profile (not shown) of the first cycle for a Li/graphite cell in a trisolvent system resembled those shown in Fig. 2. However, the amount of Chloro-EC required in a trisolvent system in order to achieve the same level of reduction in electrolyte decomposition was substantially reduced. Figure 4 shows a plot of irreversible capacity of cells cycled at a 20 h rate as a function of volume fraction of Chloro-EC in Chloro-EC/EC/PC. It is apparent that in the presence of EC the volume fraction of Chloro-EC could be reduced to as low as 0.05. We are currently carrying out experiments to determine the phase diagram of this trisolvent system, and results will be published in the near future.

Lithium-ion cells.—Cycling behavior.—A long-term cycle life study was carried out on a number of lithium-ion cells employing 1 *M* $LiClO_4$ Chloro-EC/PC (1/1) electrolyte. Under nonoptimized experimental conditions, significantly long cycle lives were observed. Figure 5 shows the potential curves for the first three charges and two discharges of a representative long cycle life cell plotted against capacity per gram of graphite. The cell is cycled at a 10 h rate. Here the $LiCoO_2$ cathode is in sufficiently large capacity excess that it is cycled over the flat region of its potential curve ($LiCoO_2$ to $Li_{0.7}CoO_2$). This makes it easier to estimate the graphite contribution to the cell-potential curve. The features of the first charge curve of this cell are similar to that of the first discharge curve of the lithium/graphite cell (cell A) of Fig. 1, but the capacity per gram of graphite is 600 as opposed to 440 mAh/g. Irreversible capacity is present on charging the cell from zero to 3.65 V. This is associated with formation of the SEI film on the graphite at potentials above 0.25 V *vs.* lithium. In the ion cell, this capacity can be estimated from the shape of the potential curve to be *ca.* 150 mAh/g as compared to *ca.* 90 mAh/g for the lithium/graphite cell. In contrast to the lithium/graphite cell, the lithium-ion cell has more capacity in the potential region of 3.65 to 3.9 V (graphite potentials between 0.25 and 0 V *vs.* lithium), usually associated with the reversible intercalation of graphite, 450 as compared to 360 mAh/g, but less reversible capacity, 290 as opposed to 360 mAh/g. This extra capacity, greater than the expected irreversible capacity for graphite and not retrievable on discharge, indicates the

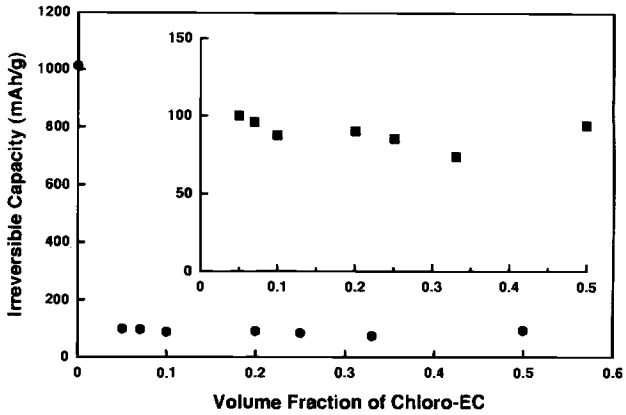

Fig. 4. Irreversible capacity of Li/KS15 graphite cells cycled at a 20 h rate as a function of the volume fraction of Chloro-EC in 1 *M* $LiClO_4$ Chloro-EC/PC/EC electrolyte where the volume ratio of EC to PC was kept at 1:1. The insert shows the same data for volume fraction 0.05 to 0.5.

Table I. Reversible capacity and capacity loss for the first cycle of lithium/KS15 graphite cells cycled at a 20 h rate employing 1 *M* $LiClO_4$ Chloro-EC/cosolvent (1/1).

Cosolvent	Reversible capacity (mAh/g)	Capacity loss (mAh/g)
PC	358	88
DMC	345	96
DEC	355	87
2Me-THF	328	172
THP	370	190
THF	365	153

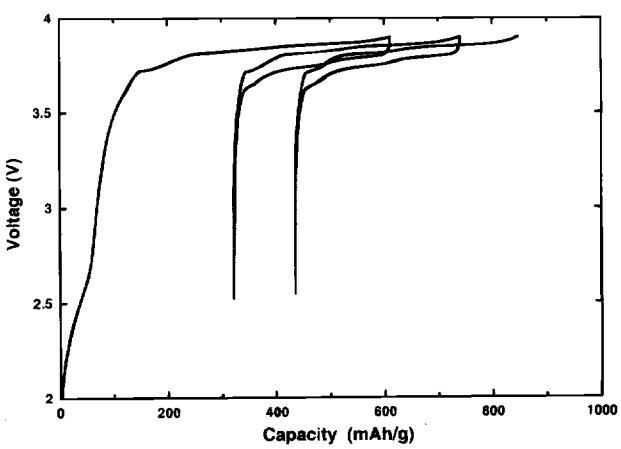

Fig. 5. Potential profiles of the first two and one-half cycles of a representative $LiCoO_2$/KS15 graphite cell employing 1 *M* $LiClO_4$ Chloro-EC/PC (1/1) electrolyte. The cell is cycled at a 10 h rate for the cycles shown. Capacity is per weight of graphite, and each cycle is plotted with a −0.2 V offset to improve clarity.

presence of a parasitic current perhaps due to a chemical shuttle. This is discussed below. The reversible cell capacity in the potential region of 3.65 to 3.9 V increases with cycle number. This can be better seen in Fig. 6 which shows a plot of discharge capacity per weight of graphite *vs.* cycle number for this representative long cycle life lithium-ion cell. The cell is cycled at a 10 h rate for the first thirteen cycles, over which the reversible capacity increases. This gradual increase in reversible capacity can be explained by at least three causes. First, it is possible that initially the cell is not completely wetted and wetting improves during these early cycles, which results in an increase in reversible capacity. Second, the SEI film formed on the surface of graphite during the first lithiation of graphite may not be complete, additional cycles being required to form completely the SEI film, especially, in the presence of a chemical shuttle where a Cl^-/Cl_2 redox couple may reduce the efficiency of the formation of SEI film (see below for further discussion of this chemical shuttle). Finally, an SEI film which takes several cycles to complete may form on the surface of carbon black (a conductivity enhancer) embedded inside the cathode.[13]

As shown in Fig. 6, the cell is then cycled at a 5 h rate for the next 383 cycles. There is an immediate decrease in capacity (from 319 to 301 mAh/g) upon the change of the cycling rate. Analysis of cell potentials immediately before and after the completion of discharge at the 5 and 10 h rate shows that this capacity decrease is a result of increased ohmic (IR) drop. The IR drop causes the potential curve to be displaced to a lower potential on discharge and to a higher potential on charge at a 5 h rate. After that, the cell capacity continued to decrease. At the end of the 396th cycle, the capacity had dropped to 211 mAh/g.

The cell was then put back to a 10 h rate. An immediate recovery of the capacity of about 13% to 238 mAh/g was obtained. Continuous cycling of the cell showed a gradual increase in capacity. At the 813th cycle, the capacity had increased to 256 mAh/g. The total loss of the capacity at the end of 813th cycle was therefore 20% of the initial capacity. At the present time, we do not understand why the cell capacity increased with cycling after the rate is decreased to the 10 h rate. Nevertheless, Fig. 6 demonstrates that a good cycle life can be obtained with Chloro-EC/PC as an electrolyte in a lithium-ion cell.

Charge efficiency.—Figure 7 shows a plot of charge efficiency as a function of cycle number for the representative lithium-ion cell described above. The charge efficiency is as defined earlier. Initially, the cell was cycled at a 10 h rate for 13 cycles, and the charge efficiency for the first cycle was relatively low, just below 50%. The charge efficiency improved over the next several cycles. The possible

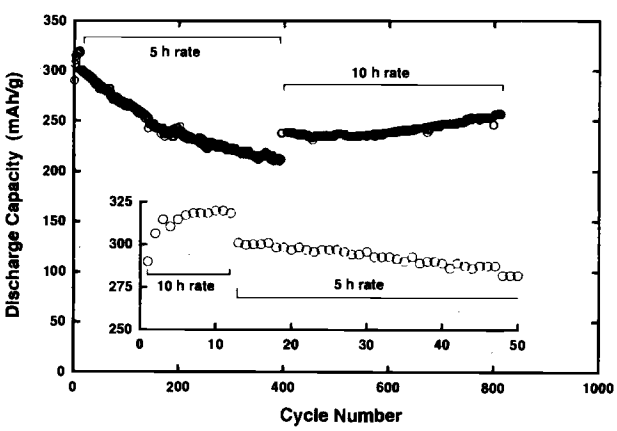

Fig. 6. A cycle life plot for the $LiCoO_2$/KS15 graphite cell of Fig. 5. The cycling rates are as shown. Capacity is per weight of graphite, and only the discharge capacity is shown. The insert shows the same data for cycle numbers 1 to 50.

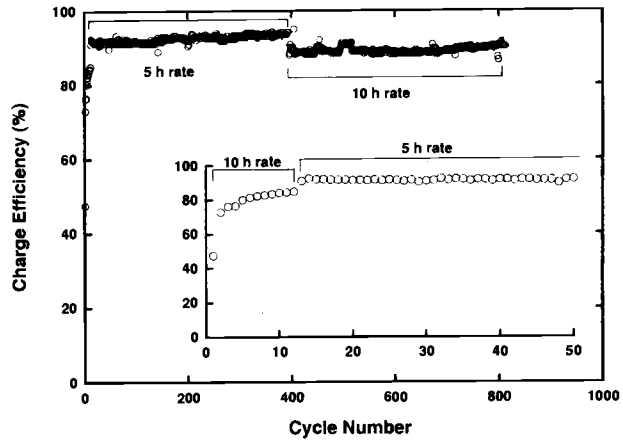

Fig. 7. A charge-efficiency plot for the $LiCoO_2$/KS15 graphite cell of Fig. 5 and 6. The insert shows the same data for cycle numbers 1 to 50.

reasons for the gradual improvement of the charge efficiency were explained above.

After ten cycles and an increase to a 5 h rate, the charge efficiency stabilized. (Charge efficiency of other cells, not shown, which were cycled at a constant rate their entire cycle life also stabilized after ten to fifteen cycles.) The cell was then cycled at this 5 h rate for the next 383 cycles. The charge efficiency was more or less constant at *ca.* 92%. Subsequently, the cycling rate was reduced to a 10 h rate for the remaining cycles; the charge efficiency decreased accordingly to about 89% but remained roughly constant.

The cycle life and charge efficiency data can be compared to data collected under similar experimental conditions for graphite/$LiCoO_2$ ion cells employing 1 *M* $LiPF_6$ in EC/DMC (1:2). Here the irreversible and reversible capacities, 80 and 340 mAh/g, respectively, were comparable to those found for 1 *M* $LiClO_4$ Chloro-EC/PC (1:1) lithium/graphite cells. Here the charge efficiency was initially 81% rising to over 98% in three cycles and over 99% in fourteen cycles. Little capacity loss to three hundred cycles was observed.

The low charge efficiency for Chloro-EC containing lithium-ion cells is unexpected as our results, given earlier for Li/graphite cells, showed initial charge efficiencies of 76 to 80% which increased ultimately to 98 to 99% within four cycles. Furthermore, the experimental conditions were the same for Li/graphite and graphite/$LiCoO_2$ cells except that the former used Li as the counterelectrode and the latter used $LiCoO_2$ as the counterelectrode. These data suggest that Chloro-EC is unstable in the presence of Li_xCoO_2 ($0.5 \leq x \leq 1.0$). However, as seen in Fig. 6, the charge efficiency stabilizes after several cycles, and the cell is able to cycle over 800 cycles without a significant capacity fade in spite of a charge efficiency of 92%. This suggests that the mechanism for the low charge efficiency is more complicated than a simple interaction between Chloro-EC and $LiCoO_2$ ($0.5 \leq x \leq 1.0$). Moreover in lithium/$LiCoO_2$ cells where the experimental conditions were the same as for the graphite/$LiCoO_2$ cells, except that the counterelectode was lithium metal, there is no indication of excessive electrolyte decomposition at the $LiCoO_2$ cathode. To 4.2 V the reversible capacity for a lithium/$LiCoO_2$ cell was found to be 125 mAh/g with an irreversible capacity of 10 mAh/g, similar to that found for $LiPF_6$ EC/DMC (1:2) electrolyte.

Preliminary investigations of the stability of 1 *M* $LiClO_4$ Chloro-EC electrolyte at high oxidation potentials were carried out using cyclovoltammetry with a Shomac 30-2 steel working electrode. In the potential range between 3.5 and 4.2 V *vs.* lithium, where the $LiCoO_2$ cathode is normally cycled in a lithium-ion cell, and 3.5 and 4.4 V *vs.* lithium, cyclovoltammetric results showed no obvious oxi-

dation or reduction peaks. Over this potential range the anodic current increased nonlinearly, but not exponentially from 0 to 4 $\mu A/cm^2$. Similar results were obtained with 1 *M* $LiClO_4$ in EC or PC although the current observed went from 0 to 8 $\mu A/cm^2$. This suggests that Chloro-EC is at least as stable as EC or PC with respect to oxidation. Similar experiments with 1 *M* $LiPF_6$ in EC/DMC (1:2) gave a current from 0 to 20 $\mu A/cm^2$. Comparable experiments were conducted with Super S carbon black working electrodes and yielded similar shaped voltammograms except that the current densities were 300 times higher due to the increased surface area of the carbon black as opposed to the Shomac steel.

If the reaction between Chloro-EC and $LiCoO_2$ was irreversible, we would not expect a long cycle life for the lithium-ion cell or the large reversible capacity of the lithium/$LiCoO_2$ cell. As shown in Fig. 5, the potential profile of a lithium-ion cell was similar in features to that of a lithium/graphite cell. The familiar potential plateau at 1.2 V (*vs.* Li) attributed to the electrolyte decomposition to form an SEI film on the graphite surface and the potential plateaus below 0.2 V (*vs.* Li) attributed to lithium intercalation are present. However, the irreversible capacity in both potential regions is larger.

Considering all the above data, the following theory for the low charge efficiency is hypothesized. During the initial lithiation of graphite, Chloro-EC which is in contact with the electrode undergoes a reductive cleavage[14] yielding LiCl and radical cations which are formed from the organic moiety. Since LiCl is only slightly soluble in our electrolyte,[15] some of it precipitates on the surface of graphite along with organic residues formed from the free-radical species. This is the formation of the SEI film. The slightly soluble LiCl can migrate to the $LiCoO_2$ electrode where it is oxidized to form Cl_2. The resultant Cl_2 can diffuse back to the lithiated anode and be reduced to Cl^-. Cl_2 and Cl^- act as an internal chemical shuttle. The net effect is equivalent to a self-discharge mechanism with a reduced charge efficiency. The shuttle does not occur with a lithium graphite cells as the lithium metal potential is too low to affect the oxidation of Cl^-. Nor is the shuttle current observable in a lithium/$LiCoO_2$ cell because the area of the lithium anode is *ca.* one-thousandths of the area of the graphite anode in the lithium ion cell. The charge efficiency and hence the magnitude of the shuttle current eventually reach a constant value as the SEI film on the graphite fully forms. The formation of this film in the lithium-ion cell is slower than in the lithium/graphite cell due to dissolution of LiCl from the film, perhaps by way of the Cl_3^- anion. The fact that the shuttle current does not go to zero indicates that the SEI film never becomes completely electronically blocking to Cl_2. The film dissolution indicated above would account for this.

This shuttle hypothesis is supported by the fact that the charge efficiency is found to be cycling-rate dependent. At a slower cycling rate, the shuttle species has more time to diffuse to the electrode and results in a smaller charge efficiency (see Fig. 7). Moreover, when fully charged cells were put on standby, the cell potential decreased from 3.90 to 3.69 V over 50 h, and the capacity of their subsequent discharge cycle was decreased. The potential decrease was judged to represent lithium composition changes in the anode and cathode as it was greater than the 100 mV change on switching from charge to discharge (see Fig. 5) and more than double that found under comparable conditions when a lithium-ion cell with 1 *M* $LiClO_4$ EC/DMC (1:2) electrolyte was put on standby. Additionally, when Chloro-EC lithium cells were put on standby at the end of discharge, the potential relaxed upward initially from 3.50 to 3.60 V and then decreased to 3.43 V after 30 h. The subsequent charge capacity was greater by *ca.* 10% than previous charge capacities. These data are consistent with the shuttle or self-discharge mechanism of Cl^- diffusing to the cathode and reducing the Li_xCoO_2 to $Li_{x+\delta}CoO_2$ and Cl_2, converting back to Cl^- at the anode with deintercalation of lithium.

If the mechanism as proposed above is correct and if Chloro-EC is replaced by Fluoro-EC, a reduction in electrolyte decomposition during the first lithiation of the graphite electrode would be expected. This is due to the smaller solubility of LiF[16] as compared to LiCl. The reduced solubility would give a lower concentration of shuttle species and consequently a lower shuttle current. This would be expected to increase the charge efficiency.

At the moment, we have not been able to identify unequivocally the chemical shuttle species. Further investigation is underway. However, the idea of the chemical shuttle does raise a very interesting point. Could it be used as an overcharge protection mechanism in a manner similar to that which presently exists in a nickel/cadmium cell? We are currently investigating this possibility.

Conclusions

A new electrolyte system containing chloroethylene carbonate and one or two cosolvents has been developed for a lithium-ion battery containing a graphitic anode. This electrolyte may in part contain propylene carbonate as a cosolvent.

In a lithium/graphite cell, the electrolyte decomposition during the first lithiation of graphite is reduced to 90 mAh/g with an electrolyte containing equal volumes of chloroethylene carbonate and propylene carbonate, dimethyl carbonate, or diethyl carbonate as a cosolvent. The volume fraction of chloroethylene carbonate can be further reduced to 0.05 in a trisolvent system with a cosolvent containing equal volumes of ethylene carbonate and propylene carbonate. The rate capability of a Li/graphite cell with a chloroethylene carbonate/propylene carbonate electrolyte shows similar results to those obtained with an ethylene carbonate/dimethyl carbonate electrolyte.

A lithium-ion cell containing chloroethylene carbonate and propylene carbonate shows a long cycle life. A capacity decrease of 20% from the initial value is observed for over 800 cycles. The charging efficiency is, however, *ca.* 80 to 90% and is dependent on rate. A self-discharge current is also present. It is hypothesized that a chemical shuttle is responsible for the low charge efficiency and cell self-discharge. The possibility of using this chemical shuttle to protect over charging a lithium-ion cell is also contemplated.

Further studies of this electrolyte with regard to low- and high-temperature performance and control of the self-discharge process are in progress.

Acknowledgment

The authors wish to thank Dr. J. Worsfold for purification of electrolyte solvents, Brenda Brouwer and Michael Hornick for technical assistance, and Lonza G + T Ltd and S. A. Ensagri-Willebroke N. V. for providing samples used in this study. Financial support from the Department of National Defense, Canada, is gratefully acknowledged.

Manuscript submitted Oct. 13, 1995; revised manuscript received March 6, 1996.

National Research Council of Canada assisted in meeting the publication costs of this article.

REFERENCES

1. M. Arakawa and J.-I. Yamaki, *J. Electroanal. Chem.*, **219**, 273 (1987).
2. A. N. Dey and B. P. Sullivan, *This Journal*, **117**, 222 (1970).
3. Z. X. Shu, R. S. McMillan, and J. J. Murray, *ibid.*, **140**, 922 (1993).
4. D. P. Wilkinson and J. R. Dahn, U.S. Pat. 5, 130, 211 (1992).
5. Z. X. Shu, R. S. McMillan, and J. J. Murray, *This Journal*, **140**, L101 (1993).
6. R. Fong, H. Al-Janby, and J. R. Dahn, U.S. Pat. 5, 028, 500 (1991).
7. J. M. Tarascon and D. C. Guyomard, Abstract 69, p. 102, The Electrochemical Society Meeting Abstracts, Vol. 93-1, Honolulu, HI, May 16-21, 1993.
8. Z. X. Shu, R. S. McMillan, and J. J. Murray, in *Rechargeable Lithium and Lithium-Ion Batteries*, S. Megahed, B. M. Barnett, and L. Xie, Editors, PV 94-

28, p. 431, The Electrochemical Society Proceedings Series, Pennington, NJ (1994).
9. Z. X. Shu, R. S. McMillan, J. J. Murray, and I. J. Davidson, *This Journal*, **142**, L161 (1995).
10. E. Peled, in *Lithium Batteries*, J.-P. Garano, Editor, p. 43, Academic Press, Inc., New York (1983).
11. R. Fong, U. von Sacken, and J. R. Dahn, *This Journal*, **137**, 2009 (1990).
12. H. Mao, P. Juric, and U. von Sacken, Abstract 38, p. 64, The Electrochemical Society Meeting Abstracts, Vol. 93-2, New Orleans, LA, Oct. 10-15, 1993.
13. D. Guyomard and J. M. Tarascon, *This Journal*, **140**, 3071 (1993).
14. J.-M. Seveant, in *Advances in Physical and Organic Chemistry*, Vol. 26, D. Bethell, Editor, p. 1, Academic Press Inc., San Diego (1990).
15. J. Butler, D. Cogley, and J. Synott, *J. Phys. Chem.*, **73**, 4069 (1969).
16. R. Jasinski, in *Advances in Electrochemistry and Electrochemical Engineering*, Vol. 8, C. W. Tobias, Editor, p. 253, Wiley-Interscience, New York (1971).

Electrochemical Insertion of Lithium into Carbon Synthesized from Condensed Aromatics

Katsuhisa Tokumitsu, Akihiro Mabuchi, Hiroyuki Fujimoto, and Takahiro Kasuh

Osaka Gas Company, Limited, Research and Development Center, 6-19-9, Torishima, Kononhana-ku, Osaka 554, Japan

ABSTRACT

The electrochemical properties of new carbon materials obtained by the heat-treatment of condensed polynuclear aromatic (COPNA) precursors have been investigated. The COPNA precursors were synthesized from an aromatic compound (pyrene, Py) and a cross-linking agent, dimethyl-*p*-xylene glycol (DMPXG), with a series of DMPXG/Py molar ratios. The results indicate that the discharge capacities of the carbons heat-treated at 800°C increased as the DMPXG/Py molar ratios increased. The discharge capacities of the carbons derived from them with molar ratios above 1.5 of DMPXG/Py were greater than 372 Ah · kg^{-1}, corresponding to the composition of stage 1 Li-GIC, LiC_6. Moreover, the discharge curves of these carbons showed two regions, one of which is the potential range of 0 to 1.0 *vs.* Li/Li^+, and the other, the plateau region around 1.0 V. The discharge capacity of the former was almost constant regardless of DMPXG/Py, whereas that of the latter increased as DMPXG/Py increased. However, the plateau region disappeared for carbon materials heat-treated above 1000°C. These results suggest that "cavities" in the carbons heat-treated below 800°C contribute to active charge-discharge of lithium species for a high-capacity carbon anode, while those in carbon materials heat-treated above 1000°C do not. Furthermore, the observed charge capacities of those carbons heat-treated in the range of 600 to 1600°C showed good agreement with the theoretical capacities calculated by using the structural parameters and the butanol displacement densities of the carbon materials. This result also supports the validity of our hypothesis, namely, that cavities in the carbon materials contribute to the charges of lithium species in lithium-ion batteries.

Introduction

Carbon materials have recently attracted attention as anodes for lithium-ion batteries because a carbon anode reduced the formation of lithium dendrites on the surface of the anode and so higher reliability and safety are obtained.[1-5] In this regard, the important issues are the improvement of these capacities and their durability. However, the electrochemical performance of carbon electrodes varies largely with different kinds of carbon, since they have a variety of structural characteristics that depend on the nature of the carbon precursors and the heat-treatment conditions. Several charge-discharge reaction mechanisms have been proposed for the anode of a lithium-ion battery using many kinds of carbons. A mechanism in which all lithium species intercalate into interlayers in the form of lithium ions and Li_2 covalent molecules with the composition of LiC_2 was proposed by Sato *et al.*[6] Zheng *et al.* reported a striking correlation between the capacity for lithium of hydrogen-containing carbons and their hydrogen content.[7] Yazami *et al.* reported a multilayer mechanism for carbon anodes with high capacities.[8] Previously we reported on the relationship between carbon structures and their capacities.[9-11] From these results we hypothesized that the capacities of the carbons with suitable cavities for the accommodation of lithium species would surpass the theoretical limit (372 Ah kg^{-1} for LiC_6 composition, because cavities in the carbons would contribute to the charge-discharge of lithium species for a lithium-ion battery. Moreover, in order to estimate the cavity amount, we have proposed a cavity index (CI), which is calculated from the structural parameters and the densities of the carbon materials, and we reported that CI values are related to the charge and/or discharge capacities of carbon anodes.[12,13]

From these results, it is possible to produce carbons with a higher capacity than those previously reported with control of the size, amount, and distribution of cavities in the carbons at will. As one method for this purpose, we investigated COPNA (condensed polynuclear aromatics) precursors using carbon anodes for lithium-ion batteries. The COPNA precursors have been first studied by Ohta *et al.* for obtaining spinnable pitches with high yield for carbon fibers.[14] The COPNA precursors are characterized by having a cross-linking structure synthesized from aromatic compounds and cross-linking agent. We thought that cavities could be formed around the cross-linking sites in the aromatic compounds during the heat-treatment of the COPNA precursors, as shown in Fig. 1. The cavities mentioned above would occur in two sites in carbon materials: (*i*) void-like sites and (*ii*) noncrystalline ones. Pursuing this idea, we examined the possibility for controlling the size, amount, and distribution of the cavities in the carbons not only by controlling the heat-treatment temperature but also by varying the proportion of the cross-linking agent *vs.* the aromatic compound.

In this paper, we report some novel results for the electrochemical properties of carbon materials obtained by the heat-treatment of COPNA precursors with various DMPXG/Py molar ratios.

Experimental

Preparation of the carbon precursor and carbon materials.—The COPNA precursors were synthesized by the reaction of pyrene (Py) and dimethyl-*p*-xylene glycol (DMPXG), which functions as a cross-linking agent. The Py/DMPXG molar ratios with 1/0.5, 1/1.0, 1/1.5, 1/2.0, 1/2.5, and 1/3.0 were given, and the amount of the catalyst, *p*-toluene sulfuric acid (PTS), was fixed at 2 weight percent (w/o) against DMPXG. The compounds of Py,